NANO LETTERS

2007
Vol. 7, No. 12
3787−3791

Morphological Control of Polar Orientation in Single-Crystal Ferroelectric Nanowires

A. Schilling,[†] R. M. Bowman,[†] G. Catalan,[‡] J. F. Scott,[‡] and J. M. Gregg*,[†]

Centre for Nanostructured Media, IRCEP, School of Maths and Physics, Queen's University Belfast, Belfast, BT7 1NN, U.K., and Department of Earth Sciences, University of Cambridge, Cambridge, CB2 3EQ, U.K.

Received September 5, 2007; Revised Manuscript Received November 7, 2007

ABSTRACT

In an attempt to explore and understand domain configurations that occur in idealized ferroelectric nanowires, a focused ion beam microscope has been used to directly cut columns in a variety of sizes from single-crystal barium titanate. The scanning transmission electron microscope has then been used to image the ferroelectric domain patterns evident after cooling through the Curie temperature in the vacuum environment of the electron microscope. As the overall length of the wires is physically constrained, the observed length-conserving packets of 90° domains with $\{110\}_{pseudocubic}$ domain-wall orientations can easily be rationalized. Such domain structures necessarily dictate that although half of the domains can be such that their polarization direction lies parallel to the axis of the wire, the other half of the domains will have polarization directions approximately perpendicular to the wire axis (nonaxial). This situation introduces a depolarizing field and associated energy, which is minimized when the nonaxial polarization is oriented perpendicular to the smallest dimension of the column. Locally changing the aspect ratio of the column dimensions therefore allows local variations in the direction of polarization to be introduced. This was demonstrated by fabricating wire structures in which dimensions were varied along their length. Such wires did indeed show morphologically controlled polar reorientation. The study suggests that shape engineering alone could be used to create complex heterogeneous dipole configurations in ferroelectrics at the nanoscale without the need for externally applied poling electric fields. Possibilities for the further development of this observation might include introducing chiral variations in wire thickness, for example, to create dipole helices.

The present roadmap for ferroelectric random access memory (FeRAM) development[1] calls for fully three-dimensional (3D) devices by 2010 with capacitor real-estate footprints of 0.03 μm^2. This drive for moving to 3D arises because of a key requirement that FeRAM capacitors must have large enough electrode surfaces to generate sufficient switched charge for the sense amplifiers to reliably discriminate between the "1" and "0" states in the memory; targeted and projected real-estate areas are not sufficient for this to be achieved using conventional 2D parallel plate capacitor arrangements, hence the imperative to move to more complex 3D structures. Schemes for 3D development include harnessing both ultralithography and self-assembly techniques[2,3] to create, for example, dielectrically coated trenches,[4,5] free-standing nanotubes,[6] ZnO nanowires,[7−9] or multiwalled carbon nanotubes (MWCNTs) conformally coated with oxides.[10] An alternative scheme is to use ferroelectric films as the gate in field effect transistors,[11,12] but these suffer from retention loss (diminishing stored charge) due to the need to ground the gate during read operations. The work at IMEC[13] and the Samsung-Tokyo Institute of Technology collaboration[14] has resulted in some commercial device-worthy parts, but at present there is no model for and little understanding of the nanodomain configurations adopted in such 3D ferroelectric devices. This is of great importance as the switching speed and operating device voltages depend upon the widths and geometries of the ferroelectric nanodomains. In the present work, we show details of domain structures in nanowires and highlight the manner in which specimen geometry can determine specific local domain configurations. Developing knowledge of this kind should help in preparing the way for the implementation of ferroelectric nanowires in 3D FeRAM memory devices.

The observation that ferroic materials of all kinds have a tendency to form into domain structures is commonplace. Domains, resulting from phase transitions from high- to low-symmetry states, form in circumstances when it is energetically favorable to minimize the macroscopic manifestation of the order parameter, or a property coupled to the order parameter, for the particular type of transition involved. In ferroelectrics specifically, because the development of spontaneous electrical polarization is coupled to physical distortion of the unit cell, domains may form either to

* Corresponding author. E-mail: m.gregg@qub.ac.uk.
[†] Queen's University Belfast.
[‡] University of Cambridge.

10.1021/nl072260l CCC: $37.00
Published on Web 11/23/2007

minimize the macroscopic charge developed at free surfaces or the macroscopic strain when cooled through the Curie temperature.[15]

The formation of domains, however, necessarily involves the creation of domain walls, which cost energy. There is therefore a balance to be found between the reduction in energy, which drives the formation of domains in the first place, and the increase in the energy of the system caused by domain wall formation. This tension has been well described in established models developed by Landau and Lifshitz,[16] Kittel,[17] Mitsui and Furuichi,[18] and Roytburd[19] in which expected ferroic domain periodicities have been rationalized in slabs of material of varying thickness. Generalizing and simplifying these models, the free energy component, which depends on the domain width (w) and thickness of slab or lamella (d), can be given as

$$G(w,d) = Uw + \frac{\gamma d}{w} \tag{1}$$

where U and γ are constants for a given system.

Considering behavior under equilibrium

$$\frac{\partial G(w,d)}{\delta w} = U - \frac{\gamma d}{w^2} = 0 \tag{2}$$

and hence

$$w = \sqrt{\frac{\gamma d}{U}} \tag{3}$$

This modeled proportionality between the domain width and the square root of the specimen thickness has been remarkably successful in matching observations, not only in bulk dimensions,[18] but in submicron thick single-crystal lamellae of $BaTiO_3$[20] and in ultrathin $PbTiO_3$ films.[21]

While the fundamental behavior of domain formation in slabs of ferroic material in which one of the physical dimensions is limited might be relatively well understood, studies of domains in ferroelectric nanowires and nanodots (dimensionally limited in more than one direction) are much less well established. A major stumbling block has been the creation of appropriate material in the first place. In 2002, Urban et al.'s report of the creation of single-crystal perovskite nanowires,[22] using solution-phase decomposition of bimetallic alkoxide precursors, allowed some initial insights to be gained.[23,24] Overall, characterization of these kinds of wires for $BaTiO_3$ has shown that they are reproducibly single crystal with one of the crystallographic axes parallel to the wire axis. This allows for the room-temperature tetragonal ferroelectric phase to possess polarization along the axis of the nanowire, and this is normally observed in the as-grown state. Local electrical poling, using scanning probe microscopy techniques, has shown that remanent polarization perpendicular to the wire axis can be induced and switched, although the stability of such perpendicular polarization is sensitive to the diameter of the nanowire and to the charge compensation conditions at the wire surface.[24] More recently lead−zirconium titanate (PZT) nanowires have been produced by electrospinning of sol−gel precursors[25] or by solution infiltration of nanoporous alumina templates.[26] Domain states appear to be less well behaved; there is a tendency for polarization to be parallel to the wire axis, but even in as-grown conditions some perpendicular polarization domains have been observed.[27]

To date, ferroelectric nanowires have been produced by controlling material growth. Here, we report observations on the domain patterns seen in ferroelectric nanowires or columns made by direct patterning of bulk single-crystal $BaTiO_3$, using a focused ion beam microscope (FIB). Domain configurations observed contrast with those seen in most studies to date and appear to result from the interplay of several factors: first, the geometry used results in constraint on the length of the nanocolumns, such that 90° shape-conserving domains form on cooling through the Curie temperature; second, only alternate 90° domains can align their polarization parallel to the axis of the nanowire, thus half of the domains possess polarization which is largely perpendicular to the wire axis (herein described generally as nonaxial), producing a depolarizing field and associated energy; third, in order to minimize depolarizing energy, domains with nonaxial polarization orient such that the polar direction is perpendicular to the smallest lateral dimension of the column. As a result, the local domain configuration is strongly sensitive to the local morphology of the nanowire. This insight not only allows for successful rationalization of domain patterns observed but also suggests that deliberately patterned morphological variations can be used to control the direction of the polarization component that is not parallel to the wire axis. Morphologically heterogeneous columns have been made that clearly demonstrate this principle.

The columns/wires of ferroelectric were fabricated from commercially obtained polished $BaTiO_3$ single crystals ($5 \times 5 \times 1$ mm^3), with $\{100\}_{pseudocubic}$ surfaces, using an FEI FIB200TEM. Initially, automated control software available on this FIB microscope was used to deposit a protective Pt bar and then to make a parallel-sided lamella with milled trenches on either side (Figure 1a,b). The orientation of the lamella was cut such that it was parallel to the side walls of the single crystal, giving one of the $<100>_{pseudocubic}$ crystallographic directions approximately perpendicular to the lamellar surface. The sample was then tilted to allow milling into the lamellar face to leave columns of material with column axes approximately parallel and perpendicular to the two $<100>_{pseudocubic}$ directions contained within the lamella, illustrated by the images in Figure 1c,d. Scanning transmission electron microscopy (STEM) using a FEI Tecnai F20 with a high-angle annular dark field detector (HAADF) allowed direct imaging of the domains present in the $BaTiO_3$. The stripe contrast seen in Figure 1e was typically initially observed with domain walls appearing to be oriented at 45° to the column axes. Such $\{110\}_{pseudocubic}$ domain wall orientation was the same as noted in previous work[28,29] and suggested that the images were of 90° domains. Because the

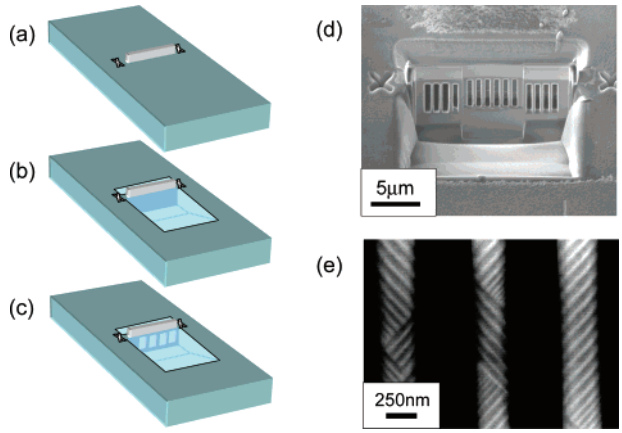

Figure 1. Schematic diagrams (a−c) illustrating the process by which the FIB microscope was used to cut nanoscale columns into $BaTiO_3$ single crystals. First, a protective Pt bar was deposited by local ion-beam induced breakdown of Pt-based organic precursor gases between two alignment crosses (a). Automated software then allowed the milling of trenches on either side of a $BaTiO_3$ lamella (b). The sample was then reoriented to allow milling into the lamellar face to leave columns of material with schematic illustration in (c), and secondary electron image in (d). STEM imaging using a high-angle annular dark field detector reveals distinct contrast from stripe domains (e).

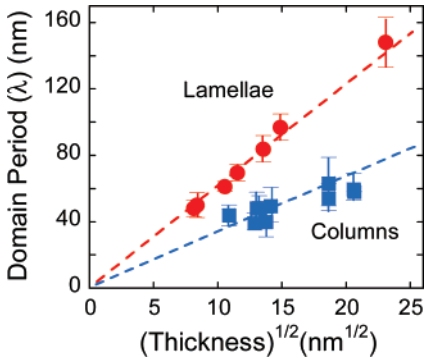

Figure 2. Measured domain period as a function of the square root of either the thickness of a $BaTiO_3$ single-crystal slab/lamella or the width of a $BaTiO_3$ single-crystal column. In both cases, the relation predicted by Kittel[17] holds, but the surface energy terms implied by the gradient in the plot are distinctly higher in the columns than in the lamellae. The ratio of slopes is very nearly 2:1, but no published theories predict this; indeed, although detailed models exist for alternating stripes of 180° domains, no published theories model zigzag arrays of 90° domains.

columns are largely length-constrained by surrounding supporting material in the lamella (Figure 1d), the formation of length-conserving 90° domains seems entirely reasonable.

Previously, the authors had investigated the manner in which the periodicity of these 90° domains changed as a function of both the thickness of a simple $BaTiO_3$ lamella[20] and the width of $BaTiO_3$ columns.[28,29] The data are summarized in Figure 2. As can be seen, a relationship between the domain period and the square root of either the thickness (in the case of the lamellae) or the width (in the case of the columns) was established, consistent with descriptions of the form of eq 3. The extent to which eq 3 should continue to be relevant as the dimensions of the ferroelectric are further reduced is an interesting issue. The derivation of the

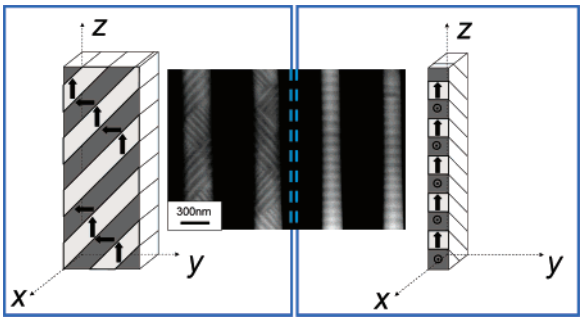

Figure 3. Schematic illustration of the domain patterns typically observed in the nanocolumns under STEM with the electron beam parallel to the *x*-axis (left). Consideration of the depolarizing energy suggests that the nonaxial component of polarization in the domains will orient approximately perpendicular to the shortest dimension in the column. Decreasing the column dimension along the *y*-axis while keeping *x* constant (right) should eventually result in a reorientation of the nonaxial polarization and an associated change in the domain contrast as viewed down the *x*-axis. The STEM image (center) illustrates that domain orientation behaves exactly as expected.

relationship assumes, among other things, that (a) ferroelectric domains consist of sets of parallel rectilinear stripes and (b) the domain wall thickness is small compared to the domain width. When either of these conditions no longer applies, the modeled relationship might be expected to break down. Very recently, Junquera and Aguado-Puente[30] have shown that (a) is not true in perovskite films thinner than three unit cells (~1.2 nm), a result that maps well to observations made on 180° domains in thin film $PbTiO_3$.[21] The relatively extended nature of the 90° domain walls relevant in our experimental work is likely to mean that assumption (b) is also no longer pertinent below dimensions of the order of a few nanometers.

Although the form of the domain periodicity behavior in $BaTiO_3$ sheets and wires in Figure 2 is similar, there is a significant difference in the gradients of the plots. Examination of eq 3 shows the gradient to be $\sqrt{\gamma/U}$, and because γ relates to the energy density of a domain wall, which is the same in both lamellae and columns, differences in the gradients of the plots in Figure 2 point only to differences in U. More specifically, the gradient differences of a factor of approximately two suggest that a domain of unit width would have a total surface-related energy four times greater in the columns than in the lamellae. The introduction of the additional surfaces associated with a column, which are not present in the lamella, is therefore relatively energetically costly.

Figure 3 (left) is a schematic illustration of the kinds of domain configurations imaged in Figure 1e and analyzed as part of the domain periodicity study. The viewing direction on STEM is along the nominal *x*-axis in the sketch. Possible polar directions associated with individual domains are added, and it is apparent that the unshaded surface perpendicular to the *y*-axis must have alternate domains with polarizations pointing directly out-of-the-surface (nonaxial). A resulting depolarizing field is expected, which is minimized when the nonaxial polarization components are perpendicular to the shortest dimension in the column.

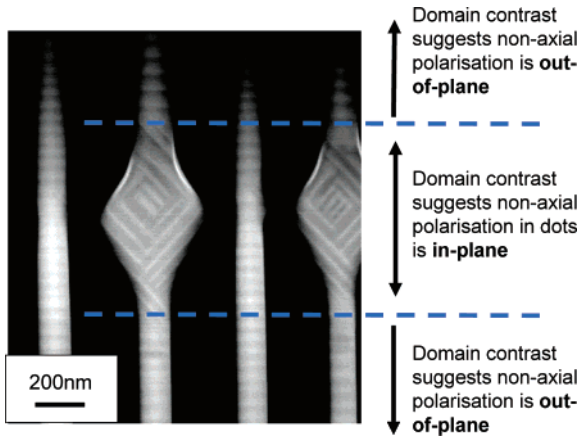

Figure 4. STEM image of FIB-cut single-crystal nanowires, which are dimensionally inhomogeneous. In general, the width of the wires is less than the thickness of the lamella from which they were cut, and hence the nonaxial component of polarization is oriented out of the plane of the micrograph, giving horizontal domain contrast. When the width of the wire is locally increased in the "dots" or "bulges" to be larger than the thickness of the lamella from which the wires were machined, the nonaxial component of polarization reorients to be in the plane of the micrograph, giving stripe domain contrast at ~45° to the wire axis. Such local control of polarization through local variation in wire morphology alone presents domain control opportunities not yet fully explored.

If this description of domain behavior is correct, then the direction of the nonaxial polarization could be rotated through 90° simply by constructing a column with a surface area perpendicular to the nominal *x*-axis smaller than that perpendicular to the *y*-axis, as illustrated on the right-hand side in Figure 3. If continuing to image along the *x*-direction, the switch in orientation of the nonaxial polarization would be manifested by a change in contrast from distinct 45° domain walls, to less distinct horizontal domain boundary contrast.

A new lamella was milled from the bulk $BaTiO_3$ crystal as before with a thickness of ~200−250 nm, and columns of different widths were cut into the lamellar face, progressively changing from column widths considerably greater than 250 nm, to widths less than 200 nm. Figure 3 (center) illustrates the dramatic change in image contrast in the columns from those with widths of ~300 nm (on the left-hand side of the STEM image), to those with widths of ~200 nm, entirely consistent with a 90° rotation of the nonaxial component of polarization in the wire. Such control of the polarization direction using relatively minor alterations in relative dimensions suggested the possibility that morphological heterogeneity might allow for shape-controlled switching along the length of an individual wire/column.

Further samples were therefore investigated in which local regions of increased width (dots) were machined in some of the wires, shown in Figure 4. In this image, the horizontal contrast indicates that the nonaxial polarization component is oriented perpendicularly to the plane of the image (as in the right-hand schematic in Figure 3), except where the local "dots" of increased width occur. Here, the contrast indicates that local 90° rotation of the nonaxial polarization has occurred from an out-of-plane orientation to an in-plane orientation. This indeed confirms that local variations in morphology along a single ferroelectric nanowire can be used to control local polar orientations. Incidentally, we also note that the in-plane domain patterns in the local dots follow closure morphology[17] to further minimize the depolarization energy. The ability to manipulate polarization behavior to this degree in the absence of patterned electrodes or an externally applied electric field seems rather exciting particularly in the context of recent atomistic simulation studies of vortex ferroelectric domain states,[31−35] and clearly further work is an imperative.

In summary, patterning of nanowires or nanocolumns from single-crystal $BaTiO_3$ has been performed using an FIB microscope, and the resulting domain configurations have been imaged using STEM. Observations suggest the following:

(i) that the specific geometry used in the study where the nanowires are length-constrained by surrounding material results in the formation of length-conserving 90° domains on cooling through the Curie temperature;

(ii) alternate domains possess polarization directions that are perpendicular to the axis of the nanowire;

(iii) the orientation of this nonaxial polarization component is strongly sensitive to local morphology to the extent that deliberate variations in the width of an individual nanowire can be used to control the local nonaxial polarization direction in a manner that can be readily understood in terms of minimization of the depolarizing field.

The authors acknowledge the Engineering and Physical Sciences Research Council and Invest Northern Ireland for financial support of the work.

References

(1) International Technology Roadmap for Semiconductors (ITRS), 2006 Update; 2006; p 23; http://www.itrs.net/Links/2006Update/2006UpdateFinal.htm.

(2) Alexe, M.; Scott, J. F.; Curran, C.; Zakharov, N. D.; Hesse, D.; Pignolet, A. Self-patterning nano-electrodes on ferroelectric thin films for gigabit memory applications. *Appl. Phys. Lett.* **1998**, *73*, 1592.

(3) Dawber, M.; Szafraniak, I.; Alexe, M.; Scott, J. F. Self-patterning of arrays of ferroelectric capacitors: description by theory of substrate mediated strain interactions. *J. Phys. Condens. Mat.* **2003**, *15*, L667−L671.

(4) (a) Menou, N.; Muller, C.; Goux, L.; et al. Microstructural analysis of integrated pin-shaped two-dimensional and three-dimensional ferroelectric capacitors from micro-focused synchrotron X-ray techniques. *J. Appl. Crystallogr.* **2006**, *39*, 376−384. (b) Menou, N.; Turquat, C.; Madigou, V.; et al. Sidewalls contribution in integrated three-dimensional $Sr_{0.8}Bi_{2.2}Ta_2O_9$-based ferroelectric capacitors. *Appl. Phys. Lett.* **2005**, *87*, Art. No. 073502.

(5) (a) Kawano, K.; Kosuge, H.; Oshima, N.; et al. Low-temperature preparation of metallic ruthenium films by MOCVD using bis(2,4-dimethylpentadienyl)ruthenium. *Electrochem. Solid-State Lett.* **2007**, *10*, D60−D62. (b) Miyake, M.; Scott, J. F.; Lou, X.; Tatsuta,T.; Tsuji, O. Misted Deposition of [3D] Trenches for DRAMs and FRAMs: I. RuO_2 Electrodes. Japan Patent Application, 2007.

(6) (a) Morrison, F. D.; et al. Ferroelectric Nanotubes. *Rev. Adv. Mater. Sci*. **2003**, *4*, 114−122. (b) Fan, H. J.; Knez, M.; Scholz, R.; et al. Influence of surface diffusion on the formation of hollow nanostructures induced by the Kirkendall effect: The basic concept. *Nano Letters* **2007**, *7*, 993.

(7) Fan, H. J.; Barnard, A. S.; Zacharias, M. ZnO nanowires and nanobelts: Shape selection and thermodynamic modeling. *Appl. Phys. Lett*. **2007**, *90*, Art. No. 143116.

(8) Kuykendall, T.; Pauzauskie, P. J.; Zhang, Y.; Goldberger, J.; Sirbuly, D.; Den-Linger, J.; Yang, P. Crystallographic alignment of high-density gallium nitride nanowire arrays. *Nat. Mater*. **2004**, *3*, 524.

(9) Nikoobakht, B.; Michaels, C. A.; Stranick, S. J.; Vaudin, M. D. Horizontal growth and in situ assembly of oriented zinc oxide nanowires. *Appl. Phys. Lett*. **2004**, *85*, 3244.
(10) Kawasaki, S. et al. arXiv:cond-mat/0706.2998 <http://xxx.lanl.gov/abs/0706.2998> and *Integr. Ferroelectr*., in press (November 2007).
(11) Okuyama, M.; Noda, M. Improvement of Memory Retention in Metal-Ferroelectric-Insulator-Semiconductor (MFIS) Structures. In *Ferroelectric Thin Films*; Okuyama, M., Ishibasji, Y., Eds.; Springer: Heidelberg, 2005; pp 219−240.
(12) (a) Ishiwara, H. Applications of bismuth-layered perovskite thin films to FET-type ferroelectric memories. *Integr. Ferroelectr*. **2006**, *79*, 3. (b) Scott, J. F. Applications of modern ferroelectrics. *Science* **2007**, *315*, 954.
(13) Goux, L.; Lisoni, J. G.; Schwitters, M.; et al. Composition control and ferroelectric properties of sidewalls in integrated three-dimensional $SrBi_2Ta_2O_9$-based ferroelectric capacitors. *J. Appl. Phys*. **2005**, *98*, Art. No. 054507.
(14) (a) Shibutani, T.; et al. Ruthenium Film with High Nuclear Density deposited by MOCVD using a Novel Liquid Precursor. *Electrochem. Solid-State Lett.* **2003**, *6*, C117−119. (b) Hoko, H.; Aoki, C.; Tabuchi, Y.; et al. Electrical properties of Pt/BLT/HfSiON/Si structure for 1T-type ferroelectric memory. *Integr. Ferroelectr*. **2006**, *79*, 105.
(15) Lines, M. E.; Glass, A. M. *Principles and applications of ferroelecrics and related materials*; Oxford University Press: Oxford, 1977; pp 87−102.
(16) Landau, L.; Lifshitz, E. Theory of the dispersion of magnetic permeability in ferromagnetic bodies. *Phys. Z. Sowjetunion* **1935**, *8*, 153.
(17) Kittel, C. Theory of the structure of ferromagnetic domains in films and small particles. *Phys. Rev*. **1946**, *70*, 965.
(18) Mitsui, T.; Furuichi, J. Domain Structure of Rochelle Salt and KH_2PO_4. *Phys. Rev*. **1953**, *90*, 193.
(19) Roytburd, A. L. Equilibrium structure of epitaxial layers. *Phys. Status Solidi A* **1976**, *37*, 329.
(20) Schilling, A.; Adams, T. B.; Bowman, R. M.; Gregg, J. M.; Catalan, G.; Scott, J. F. Scaling of Domain Periodicity with Thickness in $BaTiO_3$ Single Crystal Lamellae and other Ferroics. *Phys. Rev. B* **2006**, *74*.
(21) (a) Fong, D. D.; Stephenson, G. B.; Streiffer, S. K.; Eastman, J. A.; Auciello, O.; Fuoss, P. H.; Thompson, C. Ferroelectricity in Ultrathin Perovskite Films. *Science* **2004**, *304*, 1650. (b) Fong, D. D.; Kolpak, A. M.; Eastman, J. A.; Streiffer, S. K.; Fuoss, P. H.; Stephenson, G. B.; Thompson, Carol; Kim, D. M.; Choi, K. J.; Eom, C. B.; Grinberg, I.; Rappe, A. M. Stabilization of monodomain polarization in ultrathin $PbTiO_3$ films. *Phys. Rev. Lett*. **2006**, 96, 127601. (c) Streiffer, S. K.; Eastman, J. A.; Fong, D. D.; Thompson, C.; Munkholm, A.; Murty, M. V. R.; Auciello, O.; Bai, G. R.; Stephenson, G. B. Observation of nanoscale 180 degrees stripe domains in ferroelectric $PbTiO_3$ thin films. *Phys. Rev. Lett*. **2002**, *89*, Art no: 067601.
(22) Urban, J. J.; Yun, W. S.; Gu, Q.; Park, H. Synthesis of single-crystalline perovskite nanorods composed of barium titanate and strontium titanate. *J. Am. Chem. Soc*. **2002**, *124*, 1186.
(23) Yun, W. S.; Urban, J. J.; Gu, Q.; Park, H. Ferroelectric properties of individual barium titanate nanowires investigated by scanned probe microscopy. *Nano Lett*. **2002**, *2*, 447.
(24) Spanier, J. E.; Kolpak, A. M.; Urban, J. J.; Grinberg, I.; Ouyang, L.; Yun, W. S.; Rappe, A. M.; Park, H. Ferroelectric phase transition in individual single-crystalline $BaTiO_3$ nanowires. *Nano Lett.* **2006**, *6*, 735.
(25) (a) Wang, Z. Y.; Suryavanshi, A. P.; Yu, M.-F. Ferroelectric and piezoelectric behaviors of individual single crystalline $BaTiO_3$ nanowire under direct axial electric biasing. *Appl. Phys. Lett*. **2006**, *89*, 082903. (b) Wang, Z. Y.; Hu, J.; Yu, M.-F. One-dimensional ferroelectric monodomain formation in single crystalline $BaTiO_3$ nanowire. *Appl. Phys. Lett*. **2006**, *89*, 263119.
(26) Zhang, X. Y.; Zhao, X.; Lai, C. W.; Wang, J.; Tang, X. G.; Dai, J. Y. Synthesis and piezoresponse of highly ordered $Pb(Zr_{0.53}Ti_{0.47})O_3$ nanowire arrays. *Appl. Phys. Lett.* **2004**, *85*, 4190.
(27) Zhou, Z. H.; Gao, X. S.; Wang, J.; Fujihara, K.; Ramakrishna, S.; Nagarajan, V. Giant strain in $PbZr_{0.2}Ti_{0.8}O_3$ nanowires. *Appl. Phys. Lett*. **2007**, *90*, 052902.
(28) Schilling, A.; Bowman, R. M.; Gregg, J. M.; Catalan, G.; Scott, J. F. Ferroelectric domain periodicities in nanocolumns of single crystal barium titanate. *Appl. Phys. Lett*. **2006**, *89*, 212902.
(29) Catalan, G.; Schilling, A.; Scott, J. F.; Gregg, J. M. Domains in three dimensional ferroelectric nanostructures: theory and experiment *J. Phys.: Conden. Matter*. **2007**, *19*, 132201.
(30) Junquera, J.; Aguado-Puente, P. From 180-degree stripe domains to more exotic patterns of polarization in ferroelectric nano-structures: A first-principle view. International Conference Dynamical Properties of Solids (DyProSo XXXI), Porto, Portugal, Sept. 27, 2007; Paper IC-09.
(31) Naumov, I. I.; Bellaiche, L.; Fu, H. Unusual phase transitions in ferroelectric nanodisks and nanorods. *Nature* **2004**, *432*, 737.
(32) Kornev, I.; Fu, H.; Bellaiche, L. Ultrathin films of ferroelectric solid solutions under a residual depolarizing field. *Phys. Rev. Lett*. **2004**, *93*, 196104.
(33) Fu, H.; Bellaiche, L. Ferroelectricity in barium titanate quantum dots and wires. *Phys. Rev. Lett*. **2003**, *91*, 257601.
(34) Prosandeev, S.; Ponomareva, I.; Kornev, I.; Naumov, I.; Bellaiche, L. Controlling toroidal moment by means of an inhomogeneous static field: An ab initio study. *Phys. Rev. Lett*. **2006**, *96*, 237601.
(35) Ponomareva, I.; Naumov, I. I.; Bellaiche, L. Low-dimensional ferroelectrics under different electrical and mechanical boundary conditions: Atomistic simulations. *Phys. Rev. B*. **2005**, *72*, 214118.

NL072260L